GEOPHYSICAL RESEARCH LETTERS, VOL. 36, L13306, doi:10.1029/2009GL039167, 2009

Reply to comment by J. C. Savage on "Aseismic slip and fault-normal strain along the creeping section of the San Andreas Fault"

F. Rolandone,[1] R. Bürgmann,[2] D. C. Agnew,[3] I. A. Johanson,[2] D. C. Templeton,[2] M. A. d'Alessio,[4] S. J. Titus,[5] C. DeMets,[5] and B. Tikoff[5]

Received 13 May 2009; accepted 12 June 2009; published 14 July 2009.

Citation: Rolandone, F., R. Bürgmann, D. C. Agnew, I. A. Johanson, D. C. Templeton, M. A. d'Alessio, S. J. Titus, C. DeMets, and B. Tikoff (2009), Reply to comment by J. C. Savage on "Aseismic slip and fault-normal strain along the creeping section of the San Andreas Fault," *Geophys. Res. Lett.*, *36*, L13306, doi:10.1029/2009GL039167.

[1] Most of the relative motion between the Pacific plate and the Sierra Nevada Great Valley microplate is accommodated by strike slip along the San Andreas Fault. On the central San Andreas Fault (CSAF), the strike-slip motion occurs nearly aseismically as fault creep [*Thatcher*, 1979; *Titus et al.*, 2006; *Rolandone et al.*, 2008; *Ryder and Bürgmann*, 2008]. However, distributed contractional and right-lateral strike-slip motions also occur in the California Coast Ranges on both sides of the San Andreas. CSAF-normal convergence is accommodated on contractional structures on both sides of the fault, as evidenced by the occurrence of thrust earthquakes and Late Cenozoic uplift and folding of the Coast Ranges. A recent example of such activity is the 2003 Mw 6.5 San Simeon blind-thrust earthquake 50 km west of Parkfield [*Rolandone et al.*, 2006].

[2] The amount of strain adjacent to the creeping segment is still a matter of debate. We therefore welcome the constructive comment of *Savage* [2009] regarding our original paper [*Rolandone et al.*, 2008], which relied on GPS measurements to constrain the distribution of slip on the San Andreas Fault and quantified the deformation rates not explained by slip on major strike-slip faults. *Savage* [2009] argues that the strain-rate estimates by *Rolandone et al.* [2008] are based in part on monument velocities inferred from short runs of data spanning less than two years. He used our published station velocities to re-compute strain rates that omit such stations. We appreciate the opportunity to consider a new GPS velocity field based on data spanning longer time intervals to further improve our estimate of the strain rate adjacent to the CSAF.

[3] In his analysis *Savage* [2009] considers the central 60-km-long segment of the creeping section where data are available to calculate the strain rate for the Benito network on the NE-side of the CSAF, as well as on the SW block [*Savage*, 2009, Table 1, Figure 1]. He eliminates all the stations that were observed for less than five years, as well as monument BITT, which he considers too close to the CSAF. On the NE block, for the San Benito network, his calculation gives a resulting fault-normal (perpendicular to the average fault strike, N41°W) contraction rate of 18 ± 20 nstrain/a (when the extension rate, 3 ± 4 nstrain/a, predicted by a dislocation model of *Rolandone et al.* [2008] of deformation from SAF slip is subtracted). Across this network we reported a resulting, residual, contraction rate of 58 ± 25 nstrain/a, which is comparable to the value found by *Savage* [2009] 49 ± 27 nstrain/a when including BITT.

[4] In our paper, we discussed the role of possible anomalous site motions in our estimates of strain rate adjacent to the CSAF. We argued that removing sites from a data set (outlier removal) in such analysis should be done with caution. However, to investigate to what degree near-fault or high-residual sites impact the strain calculation, we provided (auxiliary material, Figure S3 and also readme file of *Rolandone et al.* [2008]) two evaluations for the strain rate for the NE block. Considering all the data (from the residual GPS velocities) we obtained a resulting fault-normal shortening rate 85 ± 13 nstrain/a. If we remove all sites from within 5 km of the CSAF and the PBO data (that spanned less than one year) in the interior, the strain estimate goes down to 33 ± 14 nstrain/a. For the SW block we reported a much lower value of 17 ± 12 nstrain/a [*Rolandone et al.*, 2008], a value consistent with the estimates of *Savage* [2009, Table 1]. We will therefore focus our reply on the NE block of the creeping segment.

[5] We agree with Savage's point that the most reliable strain-rate estimates are likely to come from reliable geodetic observations that span the longest time intervals. We therefore consider a new GPS velocity field that encompasses the data used in our paper (until mid-2005) and adds continuous GPS data through March of 2009 and UC-Berkeley and UW-Madison GPS data from several GPS campaigns between 2005 and 2008. Based on analysis at UW-Madison using GIPSY software, the updated velocity field for the GPS sites spanning the Coast Ranges NE of the San Andreas is shown in Figure 1 with respect to the stable Sierra Nevada – Great Valley microplate. The strain rate estimates determined from the new velocities of stations on the NE block indicate a fault-normal contraction rate of 19 ± 18 nstrain/a. The fault-normal velocity profile is shown in

[1]Institut des Sciences de la Terre Paris, UMR 7193, Université Pierre et Marie Curie, CNRS, Paris, France.
[2]Berkeley Seismological Laboratory, University of California, Berkeley, California, USA.
[3]IGPP, Scripps Institution of Oceanography, University of California, San Diego, La Jolla, California, USA.
[4]Department of Geological Sciences, California State University Northridge, Northridge, California, USA.
[5]Department of Geology and Geophysics, University of Wisconsin-Madison, Madison, Wisconsin, USA.

0094-8276/09/2009GL039167$05.00

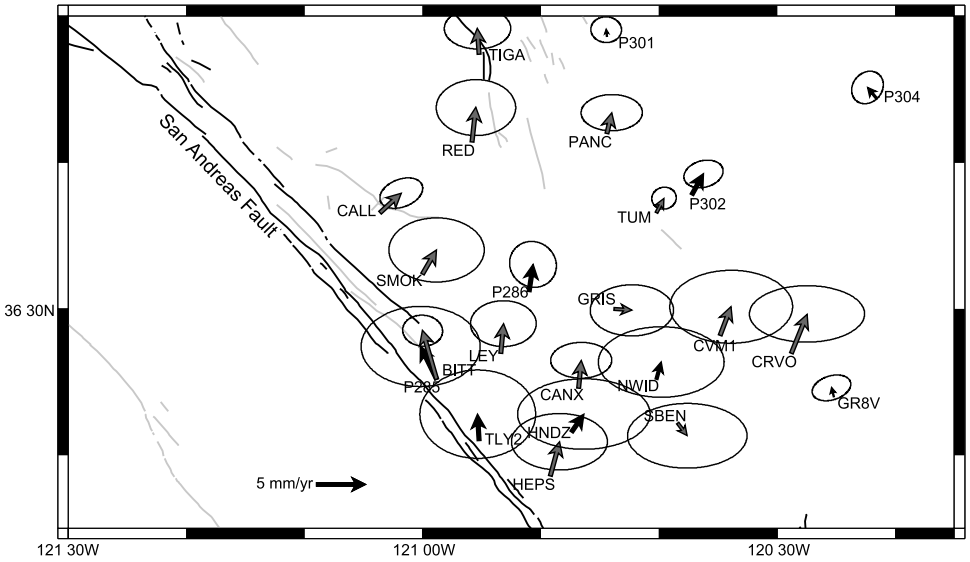

Figure 1. GPS velocities on the NE of the San Andreas fault relative to the Sierra Nevada-Great Valley microplate. Grey vectors indicate the Benito network.

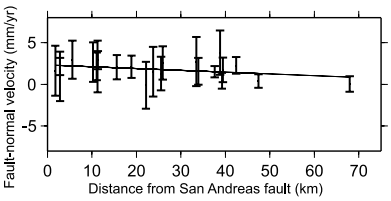

Figure 2. Plot of fault normal velocities as a function of distance from the San Andreas Fault (strike N41°W) for the sites spanning the Coast Ranges NE of the fault (as in Figure 1). The solid line shows the linear fit to the data.

Figure 2. The linear fit to the data gives 1.3 mm/yr, which over a 65 km wide zone corresponds to 20 nstrain/a.

[6] Based on his analysis of our longest GPS time series, Savage estimates that the off-fault strain rates are close to zero. Our new GPS data support his conclusion and affirm the importance of time for averaging down noise in geodetic time series, as emphasized by Savage. Efforts to measure and better understand the linkage between the small, but likely non-zero strain rates in the San Andreas fault borderlands and faulting and folding in those regions are ongoing and should benefit significantly from continued measurements at the many permanent and campaign stations now established in central California.

[7] **Acknowledgment.** This is BSL contribution 09–10.

References

Rolandone, F., D. Dreger, M. Murray, and R. Bürgmann (2006), Coseismic slip distribution of the 2003 Mw 6.6 San Simeon earthquake, California, determined from GPS measurements and seismic waveform data, *Geophys. Res. Lett.*, *33*, L16315, doi:10.1029/2006GL027079.

Rolandone, F., R. Bürgmann, D. C. Agnew, I. A. Johanson, D. C. Templeton, M. A. d'Alessio, S. J. Titus, C. DeMets, and B. Tikoff (2008), Aseismic slip and fault- normal strain along the creeping section of the San Andreas Fault, *Geophys. Res. Lett.*, *35*, L14305, doi:10.1029/2008GL034437.

Ryder, I., and R. Bürgmann (2008), Spatial variations in slip deficit on the central San Andreas fault from InSAR, *Geophys. J. Int.*, *175*, doi:10.1111/j.1365-1246X.2008.03938.x.

Savage, J. C. (2009), Comment on "Aseismic slip and fault-normal strain along the creeping section of the San Andreas Fault" by F. Rolandone et al., *Geophys. Res. Lett.*, *36*, L13305, doi:10.1029/2009GL037964.

Thatcher, W. (1979), Systematic inversion of geodetic data in central California, *J. Geophys. Res.*, *84*, 2283–2297, doi:10.1029/JB084iB05p02283.

Titus, S. J., C. DeMets, and B. Tikoff (2006), Thirty-five-year creep rates for the creeping segment of the San Andreas fault and the effects of the 2004 Parkfield eart hquake: Constraints from alignment arrays, continuous Global Positioning System, and creepmeters, *Bull. Seismol. Soc. Am.*, *96*, S250–S268, doi:10.1785/0120050811.

D. C. Agnew, IGPP, University of California, San Diego, La Jolla, CA 92093-0225, USA.

R. Bürgmann, I. A. Johanson, and D. C. Templeton, Berkeley Seismological Laboratory, 4767 McCone Hall, Berkeley, CA 94720-4760, USA.

M. A. d'Alessio, Department of Geological Sciences, California State University Northridge, 18111 Nordhoff Street, Northridge, CA 91330, USA.

C. DeMets, B. Tikoff, and S. J. Titus, Department of Geology and Geophysics, University of Wisconsin-Madison, 1215 West Dayton Street, Madison, WI 53706, USA.

F. Rolandone, Institut des Sciences de la Terre Paris, UMR 7193, Université Pierre et Marie Curie, CNRS, 4 place Jussieu, F-75252 Paris CEDEX, France. (frederique.rolandone@upmc.fr)

GEOPHYSICAL RESEARCH LETTERS, VOL. 36, L13305, doi:10.1029/2009GL037964, 2009

Comment on "Aseismic slip and fault-normal strain along creeping section of the San Andreas Fault" by F. Rolandone et al.

J. C. Savage[1]

Received 27 February 2009; revised 2 June 2009; accepted 12 June 2009; published 14 July 2009.

Citation: Savage, J. C. (2009), Comment on "Aseismic slip and fault-normal strain along creeping section of the San Andreas Fault" by F. Rolandone et al., *Geophys. Res. Lett.*, *36*, L13305, doi:10.1029/2009GL037964.

[1] *Rolandone et al.* [2008] report estimates of the strain rate adjacent to the creeping segment of the San Andreas Fault in central California. Some of their strain-rate estimates are based on monument velocities inferred from short runs of data (e. g., 2003.4–2004.8) that include coseismic corrections for the 2003.975 San Simeon and 2004.744 Parkfield earthquakes. This comment uses only the longer runs of their data for an alternative analysis that leads to strain rate estimates significantly closer to zero than they propose. In this comment tensor, not engineering, strain is used, extension is reckoned positive, and the uncertainties quoted in the text and table are standard deviations.

[2] I use data from *Rolandone et al.* [2008] to calculate the strain rate for the Benito network (the 15 monuments northeast of the San Andreas Fault in Figure 1), a network specifically chosen by *Sauber et al.* [1989] to monitor strain along the creeping section of the San Andreas Fault. The Benito network extends along the central segment of the 170-km-long creeping section of the San Andreas Fault. The velocities (Figure 1; see also yellow arrows in Figure 1 of *Rolandone et al.* [2008]) for 14 monuments (those with velocities indicated by arrows in Figure 1) in the Benito network were measured over the interval 1998.88–2004.58 [*Rolandone et al.*, 2008, Tables S1 and S3]; the velocity for monument BONT was not given. I have eliminated monument BITT from the data because it is too close (1.6 km; top of strip map C of *Brown* [1970]) to the active trace of the San Andreas Fault and thus subject to local disturbances. The positions and velocities of the remaining 13 monuments have been referred to a Cartesian coordinate system with origin at 36.21°N, 120.79°W (same origin as used by *Rolandone et al.* [2008]), the y-axis directed along the strike (N41°W) of the San Andreas Fault, and the x-axis directed perpendicular to strike (N49°E). I have then found the uniform rotation rate ω and uniform strain rates ε_{ij} that best approximate the observed velocity field according to the equations [*Jaeger*, 1964, p. 39]

$$u = u_0 + \varepsilon_{xx}x + (\varepsilon_{xy} - \varpi)y$$
$$v = v_0 + (\varepsilon_{xy} + \varpi)x + \varepsilon_{yy}y \qquad (1)$$

where u and v are the x and y components of the monument velocity, and u_0 and v_0 are constants. In the least squares solution of equation (1) for ε_{xx}, ε_{xy}, ε_{yy}, ω, u_0, and v_0 the observed velocities u and v were weighted by the inverse square of their standard deviations. The rotation and strain rates found are shown in the first entry in Table 1. (If BITT had been included in the data, the strain rates in Table 1 would have been $\varepsilon_{xx} = -46 \pm 27$. $\varepsilon_{xy} = -33 \pm 16$, and $\varepsilon_{yy} = -13 \pm 19$ nstrain/a and the rotation rate $\omega = 4 \pm 16$ nrad/a.) The standard deviations for the strain rates quoted in those tables are not the standard deviations implied by the observational error but rather are those determined from the fit of the data to the uniform deformation models. The last column of Table 1 shows the ratio of the two measures of standard deviation. The fit of the uniform deformation model to the GPS data is reasonably good: The residuals from the uniform deformation model fit are about 1.3 (last column in Table 1) times greater than the standard deviations assigned to the measurements.

[3] Other estimates of strain rate on the blocks on either side of the creeping segment of the San Andreas Fault are shown in Table 1. The second entry represents the strain rates deduced (see auxiliary material) from the changes in distances between monuments observed in the 1982.82 EDM (electromagnetic distance measurement) survey of the Benito network [*Sauber et al.*, 1989] and the subsequent 1998.88 GPS survey.[1] Figure S1 (auxiliary material) shows that the EDM strain in Table 1 does not fit the observed changes in distance very well. There are also GPS data over an interval of 5.5 or more years [*Rolandone et al.*, 2008, Table S3] for 6 monuments (CHLN, SHAD, SWTR, 0508, 0510, and 05TG; see Figure 1) on the southwestern (SW) fault block. I have used the velocities at those monuments in (1) to estimate the strain rates on the SW block (fourth entry in Table 1).

[4] I have also calculated the strain rates expected solely from steady-state slip (creep) on the San Andreas and Calaveras faults. I used essentially the same slip model (see auxiliary material) as proposed by *Rolandone et al.* [2008, Table S6] to calculate the velocities predicted by a dislocation model of the slip distribution at each of the monuments used in the GPS solutions (all of the monuments in Figure 1 except BITT and BONT).

[5] A comparison of the three essentially independent measurements (GPS and EDM for the Benito network and GPS for the SW block) of strain rate along the San Andreas Fault in Table 1 indicates general agreement among the

[1]U.S. Geological Survey, Menlo Park, California, USA.

[1]Auxiliary materials are available in the HTML. doi:10.1029/2009GL037964.

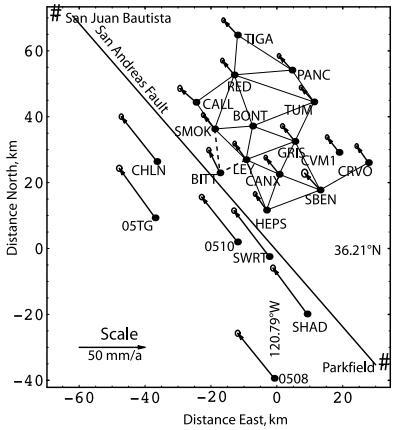

Figure 1. Map showing the creeping segment of the San Andreas Fault and the locations of survey monuments employed in the strain analysis. Monuments northeast of the San Andreas Fault constitute the Benito network. Lines joining stations in the Benito network indicate distances measured by EDM in 1982. The arrows represent velocities inferred from GPS measurements between 1998.88 and 2004.58 by *Rolandone et al.* [2008]. The error ellipses at the tips of the arrows indicate 95% confidence regions. The locations of the towns of Parkfield and San Juan Bautista are shown by the # symbols.

estimates. There is acceptable agreement between the three independent measurements of each of the strain rate components (ε_{xx}, ε_{xy}, and ε_{yy}) in Table 1, although the agreement between the GPS and EDM measurements of ε_{xx} in the Benito network is only marginal. Moreover, except for the EDM estimate of ε_{xx} in the Benito network, the observed values of strain rate are in reasonable agreement with the estimates from the dislocation model. I regard the GPS measurement in the Benito network (first entry in Table 1) as the most reliable estimate of strain accumulation along the creeping section of the San Andreas Fault. Figure S2 (auxiliary material) shows the fit of strain rates ε_{xx} in Table 1 to the GPS observed values of fault-normal displacement.

[6] The azimuth of the maximum contraction rate is directed N05°E ± 16° and N21°E ± 9° for the GPS and EDM measurements in the Benito network and N06°E ± 20° for the GPS measurements on the SW block (Table 1). The azimuth of principal contraction rate is directed ~N08°E ± 6° for the dislocation models in Table 1. *Sauber et al.* [1989] found the azimuth of the maximum contraction rate in the Benito network over the 1962–1982 interval was N16°E ± 14°. These data suggest that the axis of maximum contraction rate makes an angle of about 51° ± 4° with the strike (N41°W) of the San Andreas Fault. One might expect that the azimuth of the maximum contraction rate would be the same as the azimuth of maximum compression (i.e., stress and strain rate are coaxial). However, *Provost and Houston* [2001, Figure 8] report that the axis of principal compression makes an angle of about 82° ± 8° with the strike of the San Andreas Fault near the Benito network.

[7] The velocity of the Sierra Nevada-Great Valley microplate relative to the Pacific plate implies a normal convergence rate across the creeping section of the San Andreas Fault of 3.2 ± 0.7 mm/a (profile DD′ in Table 2 of *Argus and Gordon* [2001]). This convergence presumably is taken up by uplift of the Coast Ranges, which run along side of the fault at this latitude. If the breadth of the Coast Ranges at the latitude of the Benito network is taken as 100 km (profile DD′ in Figure 5a of *Argus and Gordon* [2001]), the average fault-normal contraction rate across the Coast Range would be 32 ± 7 nstrain/a, a value consistent with the estimates in Table 1. See *Argus and Gordon* [2001] for a more detailed discussion of the relation of this convergence to uplift.

[8] Whereas *Rolandone et al.* [2008] solved for strain accumulation rates along the entire length of the 170-km-long creeping section of the San Andreas Fault, I have considered only the central 60-km-long segment (Benito network) of the creeping section. In this way I have avoided the more complicated deformation at the ends (near Parkfield on the south and San Juan Bautista on the north) of the creeping section and taken advantage of the better data available in the Benito network. The best estimate of strain and rotation rates within the Benito network is given by the first entry in Table 1. For the Benito network the right-lateral, shear strain rate across vertical planes parallel to the San Andreas Fault was 21 ± 12 nstrain/a whereas for the larger area *Rolandone et al.* [2008] found that the right-lateral shear strain rates were <83 ± 10 nstrain/a. For the Benito network the fault-normal, extension rate ε_{xx} was −15 ± 20 nstrain/yr. If the extension rate ε_{xx} (3 ± 4 nstrain/a) predicted by the dislocation model is subtracted from that extension rate, the resulting, residual, fault-normal contraction rate is 18 ± 20 nstrain/a, which can be compared to the

Table 1. Strain and Rotation Rates (With Standard Deviations) Referred to Coordinates With y Axis Fault Parallel (N41°W) and x Axis Fault Normal (N49°E)

Network	ε_{xx} nstrain/a	ε_{xy} nstrain/a	ε_{yy} nstrain/a	ω nradians/a	Φ[a]	σ/σ_0[b]
			Benito Network			
GPS	−15 ± 20	−21 ± 12	−13 ± 13	16 ± 12	N05°E ± 16°	1.3
EDM[c]	−61 ± 17	−34 ± 14	−20 ± 16		N21°E ± 9°	2.4
Disloc. Model	3 ± 4	−28 ± 2	12 ± 3	−10 ± 2	N09°E ± 3°	0.3
			SW Block			
GPS	6 ± 56	−34 ± 29	12 ± 17	−37 ± 29	N06°E ± 20°	1.4
Disloc. Model	−5 ± 17	−33 ± 8	0 ± 5	−9 ± 9	N06°E ± 8°	0.4

[a]Azimuth of axis of the principal contraction rate.
[b]Ratio of standard deviation inferred from the uniform deformation fit to the observed standard deviation.
[c]EDM line BONT-LEY excluded.

residual, fault-normal contraction rate (85 ± 13 nstrain/a) found by *Rolandone et al.* [2008, Figure S3] near the center of the creeping section of the San Andreas Fault (i.e., within the San Benito network). Notice that *Rolandone et al.* [2008, Figure S3] find a much lower value (17 ± 12 nstrain/a) for the residual, fault-normal contraction rate on the SW fault block than on the NW fault block.

References

Argus, D. F., and R. G. Gordon (2001), Present tectonic motion across the Coast Ranges and the San Andreas fault system in central California, *Geol. Soc. Am. Bull.*, *113*, 1580–1592, doi:10.1130/0016-7606(2001)113<1580:PTMATC>2.0.CO;2.

Brown, R. D. (1970), Map showing recently active breaks along the San Andreas and related faults between the northern Gabilan Range and Cholame Valley, California, *U. S. Geol. Surv. Misc. Geol. Invest. Map.*, *I-575*.

Jaeger, J. C. (1964), *Elasticity, Fracture and Flow*, 212 pp., Methuen, London.

Provost, A.-S., and H. Houston (2001), Orientation of the stress field surrounding the creeping section of the San Andreas Fault: Evidence for a narrow mechanically weak fault zone, *J. Geophys. Res.*, *106*, 11,373–11,386, doi:10.1029/2001JB900007.

Rolandone, F., R. Burgmann, D. C. Agnew, I. A. Johanson, D. C. Templeton, M. A. d'Alessio, S. J. Titus, C. DeMets, and B. Tikoff (2008), Aseismic slip and fault- normal strain along the creeping section of the San Andreas Fault, *Geophys. Res. Lett.*, *35*, L14305, doi:10.1029/2008GL034437.

Sauber, J., M. Lisowski, and S. C. Solomon (1989), Geodetic measurement of deformation east of the San Andreas Fault in central California, in *Slow Deformation and Transmission of Stress in the Earth*, *Geophys. Monogr. Ser.*, vol. 49, edited by S. C. Cohen and P. Vanicek, pp. 71–86, AGU, Washington, D. C.

J. C. Savage, U.S. Geological Survey, MS977, 345 Middlefield Road, Menlo Park, CA 94025, USA. (jasavage@usgs.gov)